Delay Compensated Multifold Table (DCMST) Direct Power Control (DPC) with Duty Ratio Control

Abinash Rath
Department of Electrical Engg.
National Institute Technology, Rourkela
email- abinash_rath@nitrkl.ac.in

Gopalakrishna Srungavarapu
Department of Electrical Engg.
National Institute Technology, Rourkela
email-gopal@nitrkl.ac.in

***Abstract*— The DPC approach for controlling ac-dc converters has a number of benefits over traditional methods. Even with the advancement of PWM control techniques, the look-up-table based DPC presents a good substitute when a low computational load is the criteria for the system design. By using an appropriate switching table matching to the demand and eliminating the error due to control delay, the DCMST provides good steady-state performance at low computation complexity. However, as the two-level converter has a limited set of voltage vectors, the sampling frequency must be higher to ensure adequate accuracy and grid power quality. Hence this work proposes the use of multiple switching vectors in the same control period by designating one fragment of the control period for one switching vector and rest time for a zero vector to achieve improved steady-state behavior. It presents the user with a highly accurate control for an ac-dc converter at a low computational burden. The duration of the application is estimated using the power error minimization method. The performance of the proposed duty regulated DCMST-DPC is presented and compared to that of the traditional DCMST-DPC using extensive simulation study in MATLAB/Simulink.**

Keywords—Duty ratio control, Direct power control (DPC), PWM rectifier, Delay compensation, Multiple switching table

I. INTRODUCTION

Apart from the direct power control in the past, many control techniques like voltage-oriented control, sine PWM, current hysteresis, etc., have been employed for the control of the PWM rectifier to convert the ac power to dc power for various domestic and industrial applications. Instead of using the converter side voltage or the source current phasor as the control variable of interest for the operation of the PWM rectifier, T. Noguchi used the converter's momentary active and reactive powers as a control parameter [1] and named it as the direct power control. The DPC approach, on the other hand, has various benefits over the other control methods, including accurate output voltage control, high power factor, and less distortion in the source current waveform.

The DPC, which is equivalent to direct torque control in motor drives, is a high-performance control technique for PWM rectifiers. The DPC, unlike the VOC, selects the required voltage vector from a defined switching table, overcoming the internal current loop. However, in a typical DPC, the switching table is constructed heuristically, which cannot guarantee the optimality of the chosen voltage vector. Some authors have proposed novel switching tables to increase performance over the typical switching table. The employment of fast and slow tables, depending on the nature of demand, enhances dynamic speed and limits the switching loss [2], [3]. The performance up-gradation, however, is restricted since the entire its subsequent attributes are not considered.

The orthodox ST-DPC still finds its application in a situation where the low algorithm complexity of the control method is a priority over the extra accuracy of the advanced modern DPCs. As a result, an algorithm-based vector selection approach [4] uses an adjustable switching table to cope with the challenges involved with the traditional ST-DPC's use of a static lookup table. Recognizing the importance of a simplified control scheme, a blend of the predictive attribute with ST-DPC by compensating for the inescapable control delay inherent in the physical system is presented in [3]. As a result, a vastly accurate control algorithm having less execution time has evolved that can be implemented in a low-cost processing unit.

The introduction of duty cycle control (in which each control cycle comprises of a non-zero switching vector succeeded by a zero switching vector) to the traditional DPC in [1] greatly eliminates power ripples and refines the source current waveform while maintaining stability [5]. The use of active vectors or the null vector as the second switching voltage vector decreases the ripple in the control variables even more, as stated in the ripple reduced Model Predictive DPC [6]. Obtaining a duty ratio that is negative or larger than unity is one of the major difficulties that causes spikes in the current and power waveforms in these duty ratio-based control approaches. The duty cycle computation procedure is updated in [7] to solve this issue.

During a single control period, a conventional DCMST-DPC uses only one voltage vector. Yet, just using one voltage vector during a single control cycle does not fully use the DCMST-DPC's potential for optimizing steady-state performance. Additionally, the performance boost achieved by the DCMST-DPC is restricted as a consequence of the limited pool of available voltage vectors in the given converter topology, and the sampling frequency should be large to assure optimum performance. Many control systems, in contrast, employ three voltage vectors within a single control period to produce diminished ripples and a constant switching frequency. Despite the fact that the three-vector-based control has higher steady-state performance and at a lower sampling rate, it is usually not preferred as the vector selection is too complex. This work presents the duty control idea in the DCMST-DPC to improve control accuracy over the traditional single-vector-based DCMST-DPC.

978-1-6654-7124-4/22/$31.00 ©2022 IEEE

II. System Modelling

A pulse width modulated three-phase converter bridge attached to the grid with resistance *R* and filtering inductance *L* is depicted in Fig. 1.

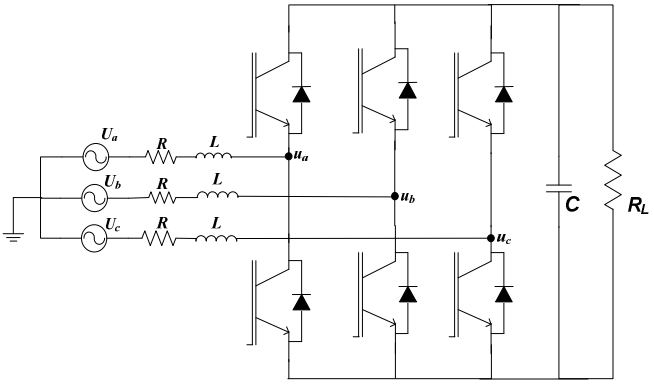

Fig. 1. A circuit showing the power converter, grid, and the load

The difference between the grid voltage vector '*U*' and the converter side space vector '*u*' can be given as shown in (1).

$$U - u = iR + L\frac{di}{dt} \tag{1}$$

By reorganizing and obtaining the conjugate of both sides of (1), the following relationship can be derived as shown in (2).

$$\frac{di^*}{dt} = \left(U^* - u^* - i^* R\right) \times \frac{1}{L} \tag{2}$$

Where the vector *u* can be expressed as shown in (3).

$$u = \frac{2}{3}\left|U_{dc}\right| \exp\left[j(v-1)\frac{\pi}{3} \right] \tag{3}$$

The *pq* theory states, if the instantaneous active power is *p*, the reactive power is *q*, and the conjugate operator is "*" the correct expression for the instantaneous complex power drawn from the grid is given by the expression as shown in (4).

$$s = p + jq = \frac{3}{2}\left(i^* U\right) \tag{4}$$

The basic control approach of the DPC is built upon the gradients of the active and reactive power. Hence it is important to have their mathematical expression. These expressions can be obtained by differentiating (4) to obtain (5) and separating their respective real and imaginary parts as shown in (5).

$$\frac{dp}{dt} + j\frac{dq}{dt} = \frac{3}{2}\left(\frac{di^*}{d} U + \frac{dU}{d} i^* \right) \tag{5}$$

When three phases of the grid voltage are balanced, the grid voltage gradient may be defined as displayed in (6). Here ω represents the angular frequency of the vector *U*.

$$\frac{d}{dt}\left(U\right) = j\omega U \tag{6}$$

Using (2), (3), and (6) in (5), the final expressions for the active and reactive power gradients for v^{th} active switching vector can be obtained as shown in (7). For the zero vector, the power gradients are denoted as $\dot{p}_0$ and $\dot{q}_0$. These zero vector gradients are expressed as shown in (8).

$$\left.\begin{aligned} \dot{p}_v &= 1.5\frac{\left|U\right|^2}{L} - \frac{\left|U\right|\left|U_{dc}\right|}{L}\cos(\omega t - (v-1)\frac{\pi}{3}) \\ \dot{q}_v &= \omega p - \frac{\left|U\right|\left|U_{dc}\right|}{L}\sin(\omega t - (v-1)\frac{\pi}{3}) \end{aligned}\right\} \tag{7}$$

$$\left.\begin{aligned} \dot{p}_0 &= 1.5\frac{\left|U\right|^2}{L} \\ \dot{q}_0 &= \omega p \end{aligned}\right\} \tag{8}$$

The maximum values of $\dot{p}_v$ and $\dot{q}_v$ which can be obtained using (7) are represented by variables $\dot{p}_{\max}$ and $\dot{q}_{max}$ respectively which can be obtained by replacing the cos ψ and sin ψ in (7) with -1. Where,

$$\psi = \omega t - (v-1)\frac{\pi}{3} \tag{9}$$

$$\left.\begin{aligned} \dot{p}_{\max} &= \frac{3\left|U\right|^2}{2L} + \frac{\left|U_{dc}\right|\left|U\right|}{L} \\ \dot{q}_{\max} &= \omega p + \frac{\left|U_{dc}\right|\left|U\right|}{L} \end{aligned}\right\} \tag{10}$$

The numeric values of the $\dot{p}_v$ and $\dot{q}_v$ are not represented in their absolute units to present the reader a better understanding of the degree to which a certain switching combination impacts the active and reactive power consumption by the converter, here in this work, a standardized formulation is utilized. The active and reactive power slopes are given as a proportion of the greatest respective power gradientss obtained in the normalized expression, regardless of the switching vector and the phase angle ωt.

$$\dot{p}_{v,nor} = \frac{\dot{p}_v}{\dot{p}_{\max}} \qquad \dot{q}_{v,nor} = \frac{\dot{q}_v}{\dot{q}_{\max}} \tag{11}$$

Fig. 2 depicts the characteristics of all possible switching combinations according to how their respective values of $\dot{p}_v$ and $\dot{q}_v$ the change with respect to change in the phase angle (ωt). Fig. 2 (a) shows that for every given sector, certain sets of switching vectors increase active power consumption while others decrease it. A similar effect may be seen in Fig. 2 (b) with the reactive power slopes.

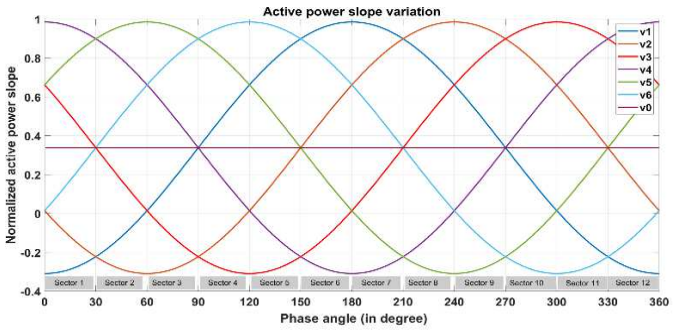

(a)

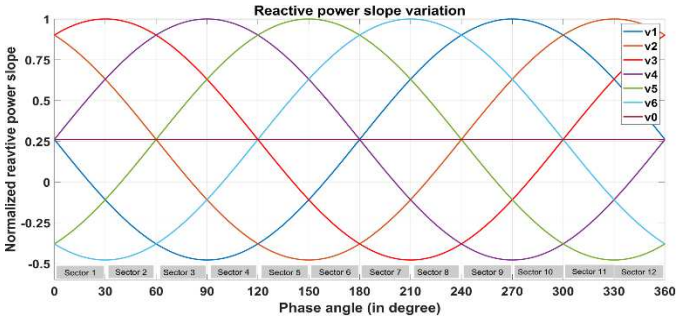

(b)

Fig. 2. Waveforms of $\dot{p}_v$ and $\dot{q}_v$ with respect to the phase angle of the grid

III. Delay Compensated Multifold Table DPC with Duty Ratio Control

The construction of the different lookup tables are based upon the curves presented in Fig. 2. The fast table, shown in Table I, is created by identifying the switching voltage vector that delivers the maximum values of active and reactive power gradient in the required polarity as determined by the hysteresis controllers. Similarly, Table II corresponds to the slow switching table which is constructed by selecting the vectors that produce lesser values of $\dot{p}_v$ and $\dot{q}_v$ in a given sector. For the selection of the final switching vector, a combination of both tables is used depending upon the magnitude of the requirement [3].

TABLE I. Fast switching table for DCMST-DPC [3]

Errors		Sector (y)											
S_p	S_q	1	2	3	4	5	6	7	8	9	10	11	12
0	0	V_1	V_1	V_2	V_2	V_3	V_3	V_4	V_4	V_5	V_5	V_6	V_6
0	1	V_1	V_2	V_2	V_3	V_3	V_4	V_4	V_5	V_5	V_6	V_6	V_1
1	0	V_5	V_6	V_6	V_1	V_1	V_2	V_2	V_3	V_3	V_4	V_4	V_5
1	1	V_4	V_4	V_5	V_5	V_6	V_1	V_1	V_2	V_2	V_3	V_3	V_4

TABLE II. Slow switching table for DCMST-DPC [3]

Errors		Sector (y)											
S_p	S_q	1	2	3	4	5	6	7	8	9	10	11	12
0	0	V_1	V_1	V_2	V_2	V_3	V_3	V_4	V_4	V_5	V_5	V_6	V_6
0	1	V_2	V_2	V_3	V_3	V_4	V_4	V_5	V_5	V_6	V_6	V_1	V_1
1	0	V_5	V_6	V_6	V_1	V_1	V_2	V_2	V_3	V_3	V_4	V_4	V_5
1	1	V_7	V_7	V_0	V_0	V_7	V_7	V_0	V_0	V_7	V_7	V_0	V_0

Owing to mutual interference, it is extremely difficult to provide total controllability of both p and q concurrently. Because most DPC applications set 'Q_{ref}' to '0' merely to obtain unity power factor, the converter's rapid transient performance may be attained by employing a voltage vector that creates the largest 'p' gradients. As a result, the type of lookup table to be utilized is determined by the amount of the active power error. When the difference of active power p and the P_{ref} is less than 'x', the slow table is used else the fast table is used.

$$x = (\dot{p}_{\max} \times T_s) \times 50\% \tag{12}$$

When the error is more than 'x' the slow table fails to supply the requisite power gradient because it usually employs switching vectors with a $\dot{p}_v$ of less than 50% of $\dot{p}_{\max}$. The switching loss increases as the value of 'x' decreases. Using a greater value of 'x', on the other hand, has a detrimental impact on converter performance since the switching vector choice is no longer in agreement with the desirable extent of demand, making the system equivalent to the standard DPC in [1]. As a result, choosing the value of the hysteresis band is always an agreement between the losses occurring because of switching and the performance of the converter [3].

For gathering the sensor input data, evaluating the control procedure, and producing the required output as the switching vector to be fed to the converter, a certain execution time is required. A control delay is employed for this purpose, giving the CPU a time period equivalent to one sample period for the complete data transfer and execution. On the other hand, using this delay block prevents the control process's switching vector from being applied to the converter immediately. Only the '$(k+1)^{th}$' instant can use the vector prescribed at the 'k^{th}' instant causing inaccuracy.

To overcome this problem, the DCMST-DPC moves the controller act to the next instant of sampling. The error at the '$(k+1)^{th}$' moment is used by the controller to determine the vector for 'k^{th}' sampling. The used switching vector (n) at the preceding sampling instant, as well as other circuit characteristics, are used to forecast future instantaneous powers analytically. The expected active and reactive powers (p_{k+1}, q_{k+1}) after the use of switching vector combination are presented in mathematical formulae (13).

$$\begin{bmatrix} p_{k+1} \\ q_{k+1} \end{bmatrix} = \begin{bmatrix} p_k \\ q_k \end{bmatrix} + \begin{bmatrix} \dot{p}_{k-1} \\ \dot{q}_{k-1} \end{bmatrix} dT_s + \begin{bmatrix} \dot{p}_0 \\ \dot{q}_0 \end{bmatrix} (1-d)T_s \tag{13}$$

Where d represents the duty ratio.

A. Duty Ratio Control

In single vector control approaches the controller has the freedom only to choose one vector for the regulation of the control variables. With the addition of the duty ratio control, now the controller can apply multiple switching combinations in a control period to accurately follow the command signal. Because active power is more of a priority in this study, duty d will be used to improve active power's satisfactory performance [5].

In an ideal case, it can be said that the controller is able to match the control variable 'p' with its reference P_{ref} perfectly.

This can be mathematically presented as shown in the (14), where, '*n*' represents the switching voltage vector selected from the DCMST control algorithm.

$$P_{ref} = p + \dot{p}_n \times dT_s + \dot{p}_0 \times (1-d)T_s \tag{14}$$

By simplifying (14), an expression for the duty ratio (*d*) is framed which is shown in (15).

$$P_{ref} - p - T_s\dot{p}_0 = (\dot{p}_n - \dot{p}_0) \times dT_s$$

$$d = \frac{P_{ref} - p - T_s\dot{p}_0}{T_s(\dot{p}_n - \dot{p}_0)} \tag{15}$$

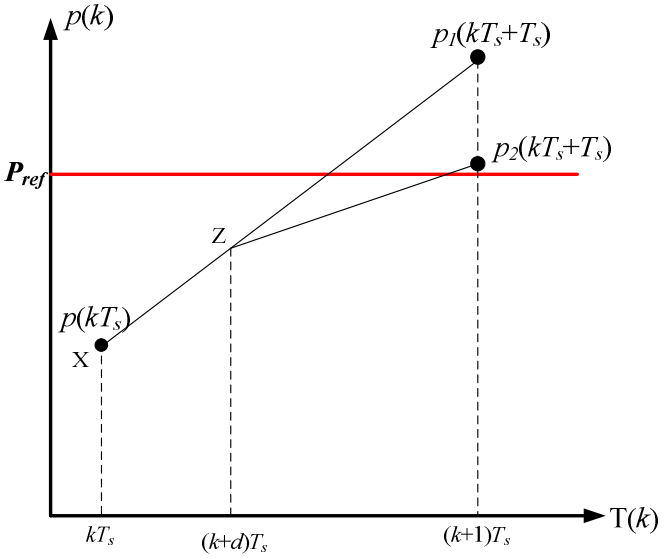

Fig. 3. Illustration of duty ratio control

To illustrate the concept of the duty cycle, let's consider which represents the instantaneous active power on the vertical axis and the discrete time scale on the horizontal axis as shown in Fig. 3. X is the point representing the instantaneous active power at k^{th} sampling instant which is represented as kT_s on the time axis. As the orthodox single vector approach uses only one switching vector throughout the duration of time from kT_s to $(k+1)T_s$, it takes the active power level to $p_1(kT_s + T_s)$ which is seen to have a greater vertical distance from the desired value of P_{ref}. But when the duty ratio concept is used, the switching vector selected at the beginning of the control period is no longer applied till the end, rather at the point Z the controller applies the zero vector which has a positive active power slope at a smaller magnitude. Proper calculation of the value of *d* results in an active power level of $p_2(kT_s + T_s)$ at the end of the control period. The $p_2(kT_s+T_s)$ can be observed to be very close to the required value of P_{ref}. In this way, the duty-controlled DPC methods are flexible to operate with any desired value of average active power slope which can be used to exactly track the command at the completion of the control period in contrast to the fixed active power slope of the vector decided by the controller.

It must be remembered that during a dynamic process, the value of dT_s may surpass the control period T_s or be negative. To ensure system dynamic stability, only the non-zero vector will be used throughout the control period [5]. The proposed idea of duty-controlled DCMST-DPC is represented in blocks in Fig. 4.

IV. Results

A two-level PWM rectifier is digitally simulated in the MATLAB/Simulink test the efficacy of the proposed work. Comparative results are presented which are obtained by the proposed method and the single vector mode of DCMST-DPC described in [3]. For both the methods the circuit parameters along with other model parameters are kept identical. In this comparative study both the simulation models are evaluated for a control period which spans out for a duration of 100 µs.

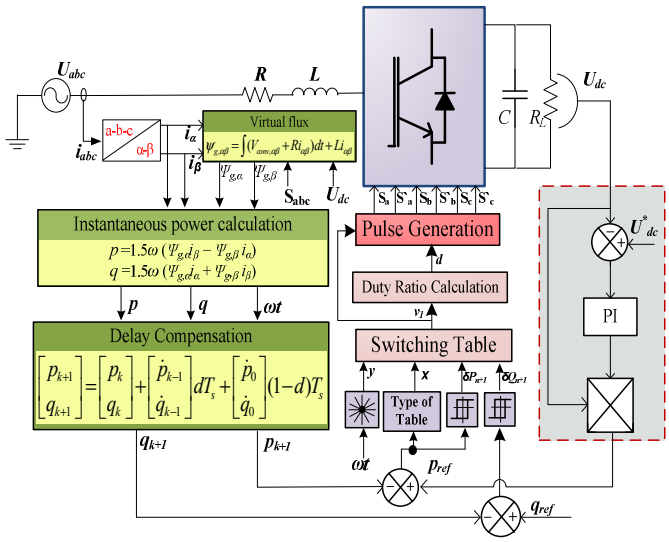

Fig. 4. Block diagram of the recommended controller

The source-side voltage, current the load side voltage, and the instantaneous powers drawn from the source are shown in Fig. 5 and Fig. 6 in the given order for the different active power levels of 540 W and 1080 W at which the PWM rectifier is operated. Fig. 5 (a) and Fig. 6 (a) correspond to DCMST-DPC and Fig. 5 (b) and Fig. 6 (b) represent the waveforms obtained from the proposed method. It can be observed from both Fig. 5 and Fig. 6 that even at different active power levels the waveforms of the source current are much smoother than the existing method and its shape is closer to the perfect sinusoidal waveform in the case for the proposed method for the same supply voltage. The THD of the source current waveform obtained with the proposed method is 5.53% and 3.75% for an active power of 540 W and 1080 W respectively which is almost 50% of the value obtained from DCMST-DPC. The detailed harmonic spectrum for the input current are shown in Fig. 7.

From the waveforms of the dc-link voltage shown in Fig. 5 and Fig. 6, it can be observed that the proposed method makes the control more accurate by not allowing U_{dc} to drift from its reference of 180 V. To quantify the drift from the reference variance is evaluated from the U_{dc} samples that are collected over a duration of 1 s. The obtained variance are tabulated in TABLE III. Both methods appear to maintain *p* and *q* about their respective references. However, large fluctuations of *p* and *q* can be observed in the case of the conventional method which

appear to be reduced with the proposed method. For the quantitative analysis, the ripple content in the p and q waveform are evaluated from the samples of p and q and tabulated in TABLE III. A large reduction in the active power (70%) and reactive power ripple (35%) can be can be observed from TABLE III. for R_L equal to 60 Ω. For 30 Ω load resistance, the active power ripple reduction and reactive power ripple reduction are found to be 59% and 24% respectively.

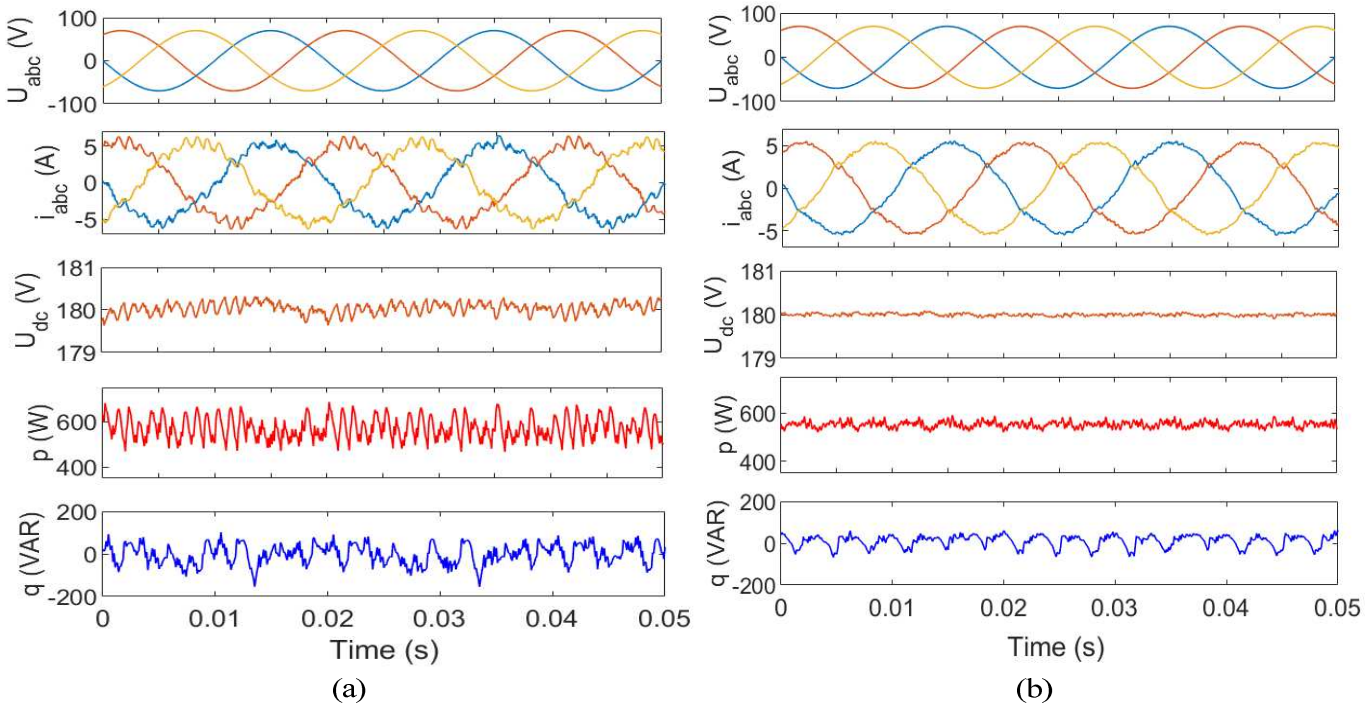

Fig. 5. Waveforms of source voltage (U_{abc}), source current (i_{abc}), dc link voltage (U_{dc}), instantaneous active power (p), and instantaneous reactive power (q) with load resistance of 60 Ω for (a) DCMST-DPC (b) Proposed method

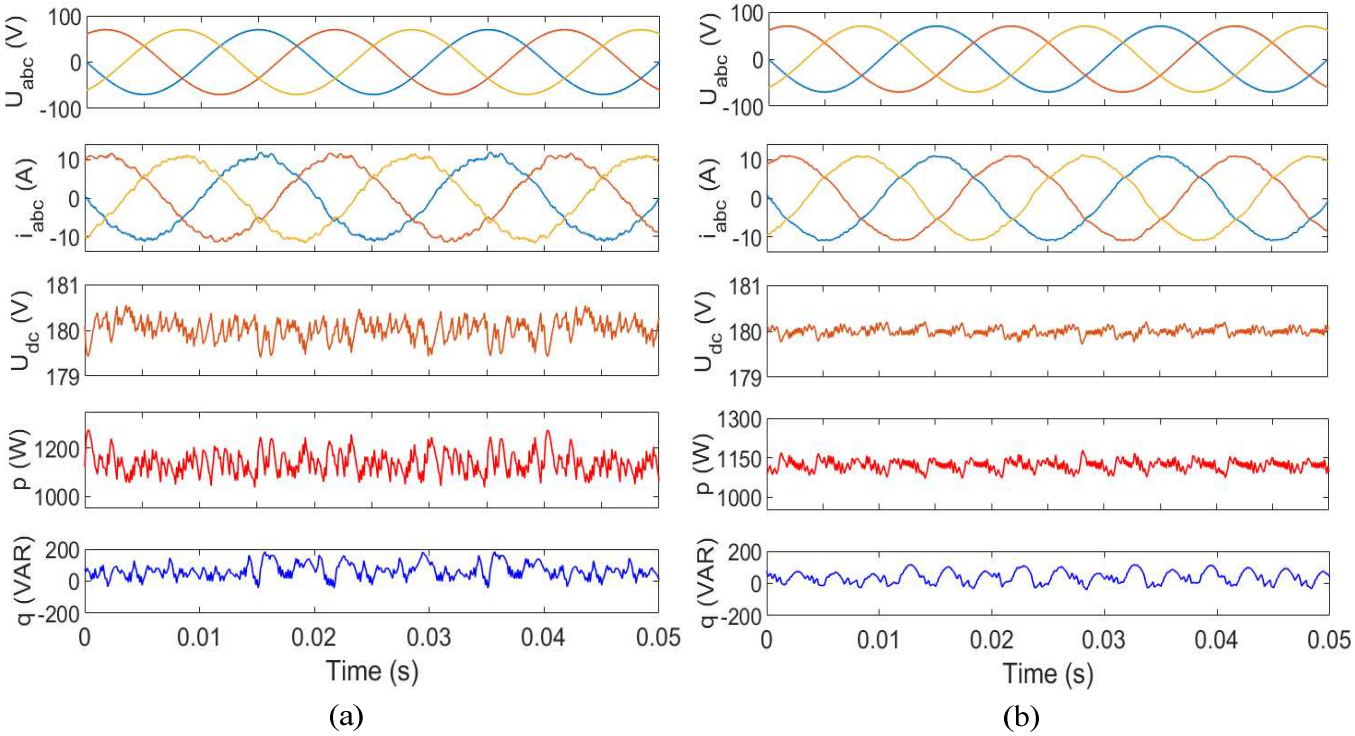

Fig. 6. Waveforms of source voltage (U_{abc}), source current (i_{abc}), dc link voltage (U_{dc}), instantaneous active power (p), and instantaneous reactive power (q) with load resistance of 30 Ω for (a) DCMST-DPC (b) Proposed method

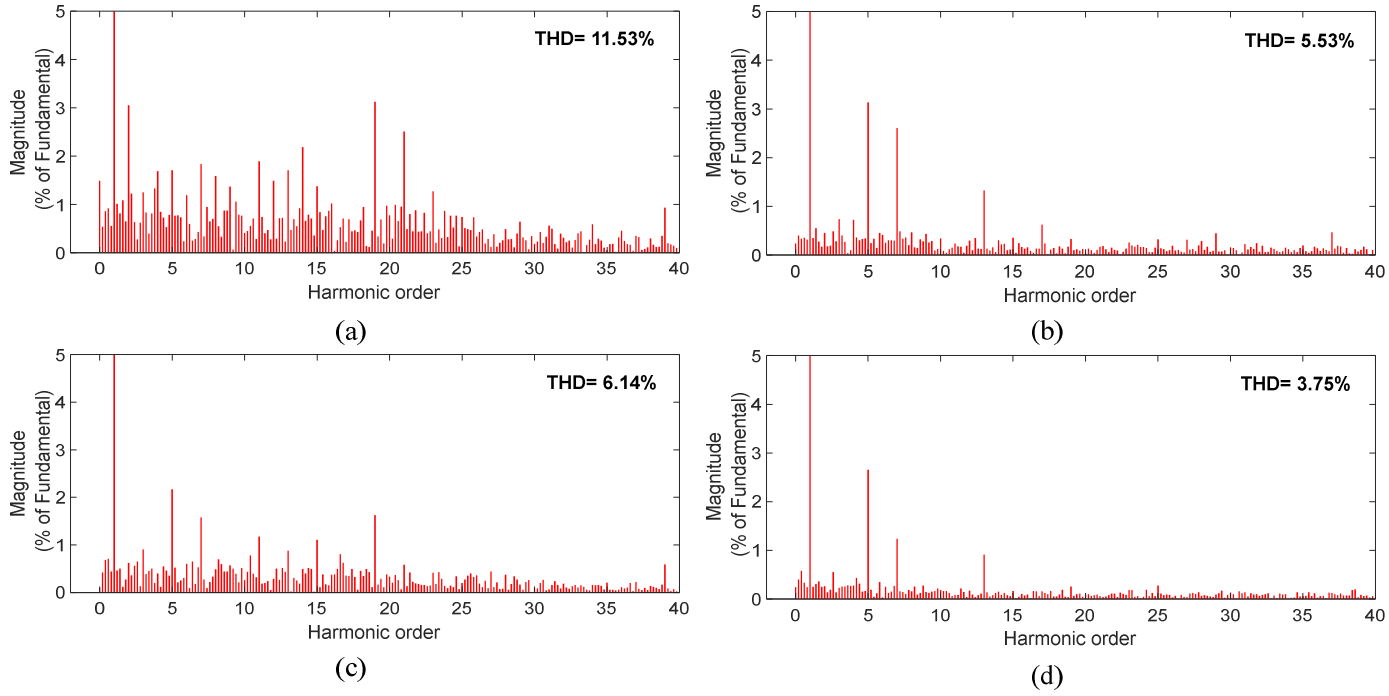

Fig. 7. Source current spectrum for (a) DCMST-DPC at 60 Ω (b) Proposed method at 60 Ω (c) DCMST-DPC at 30 Ω (d) Proposed method at 30 Ω

TABLE III. COMPARISON OF PERFORMANCE INDICES

Index	DCMST-DPC (R_L=60 Ω)	Proposed-DPC (R_L=60 Ω)	DCMST-DPC (R_L=30 Ω)	Proposed-DPC (R_L=30 Ω)
THD (%)	11.42	5.53	6.18	3.75
P_{rip} (W)	47.58	14.49	48.03	20.42
Q_{rip} (Var)	47.04	28.83	48.31	36.88
$(U_{dc})_{var}$ (mV)	17.455	1.237	52.595	8.536

V. CONCLUSION

This paper has proposed the use of the duty ratio control with the DCMST-DPC to make it a two vector switching in comparison to the single vector operation in existing DCMST-DPC. From the results section, the obtained performance parameters prove the superior control of the proposed method over DCMST-DPC in the steady state. The obtained line current THD are reduced to its 50% at different active power levels. Similarly a large improvement in the ripple content of the instantaneous active and reactive power can also be observed. Hence, it can be said that the proposed method provides the user a great advantage of high grid power quality and accurate control of instantaneous powers at low computation complexity. However, as the proposed method uses expressions of duty cycle which are dependent on circuit or model parameters, the accuracy may degrade slightly when the operating circuit and model parameters greatly differ from the values known to the user. So as a future work the inductance estimation can be a good option to have a better performance.

REFERENCES

[1] T. Noguchi, H. Tomiki, S. Kondo, and I. Takahashi, "Direct power control of PWM converter without power-source voltage sensors," *IEEE Trans. Ind. Appl.*, vol. 34, no. 3, pp. 473–479, 1998, doi: 10.1109/28.673716.

[2] J. G. Norniella *et al.*, "Multiple switching tables direct power control of active front-end rectifiers," *IET Power Electron.*, vol. 7, no. 6, pp. 1578–1589, 2014, doi: 10.1049/iet-pel.2013.0492.

[3] A. Rath, G. Srungavarapu, and M. Pattnaik, " An advanced virtual flux integrated multifold table-based direct power control with delay compensation for active front-end rectifiers ," *Int. Trans. Electr. Energy Syst.*, no. October, pp. 1–22, 2021, doi: 10.1002/2050-7038.13174.

[4] A. Rath, A. Kumar, G. Srungavarapu, and M. Pattnaik, "Power quality improvement using 18 sector algorithm based direct power control," *Int. Trans. Electr. Energy Syst.*, no. April 2020, pp. 1–17, 2021, doi: 10.1002/2050-7038.12784.

[5] Y. Zhang, Z. Li, Y. Zhang, W. Xie, Z. Piao, and C. Hu, "Performance improvement of direct power control of pwm rectifier with simple calculation," *IEEE Trans. Power Electron.*, vol. 28, no. 7, pp. 3428–3437, 2013, doi: 10.1109/TPEL.2012.2222050.

[6] H. Fang, Z. Zhang, X. Feng, and R. Kennel, "Ripple-reduced model predictive direct power control for active front-end power converters with extended switching vectors and time-optimised control," *IET Power Electron.*, vol. 9, no. 9, pp. 1914–1923, 2016, doi: 10.1049/iet-pel.2015.0857.

[7] M. Li, X. Wu, S. Huang, and G. Liang, "Model predictive direct power control using optimal section selection for PWM rectifier with reduced calculation burden," *Int. J. Electr. Power Energy Syst.*, vol. 116, no. July 2019, p. 105552, 2020, doi: 10.1016/j.ijepes.2019.105552.